# Naphthalimide-derived Chemosensor for Ratiometric Detection of Sulphide Ions: Insights into $S^{2-}$ Driven Reduction Cascade; Real-time Applications and Live Cell Imaging of Bacterial Cells

Saurabh Gupta,[a,b] Gulshan Kumar,[c] Vijay Luxami,[a] Kamaldeep Paul[a,b]*

[a]Department of Chemistry and Biochemistry, Thapar Institute of Engineering and Technology,

Patiala-147004, India

[b] TIET-VT, Centre of Excellence in Emerging Materials, Thapar Institute of Engineering and Technology, Patiala, Punjab, India-147004

[c]Department of Chemistry, Banasthali University, Banasthali Newai 304022, Rajasthan, India

*Email: kpaul@thapar.edu

**Table of Contents**

## Materials and Methods

The chemicals used to synthesize compound **NATRP** were obtained from different suppliers, namely Sigma Aldrich Ltd., Loba Chemie and Spectrochemical, based on their availability. All solvents employed in the synthesis were of spectroscopic grade and were used without purifications. The reactions were monitored with thin-layer chromatography using silica plates coated with silica gel GF-254. UV light (254 or 365 nm) was used to analyze the changes in TLC. The compounds were purified by column chromatography using silica gel (60-120 mesh). The $^{1}$H NMR and $^{13}$C NMR spectra were recorded on BRUKER ECS-400 MHz spectrometer at room temperature ($^{1}$H NMR at 400 MHz and $^{13}$C NMR at 100 MHz). NMR samples were prepared in $CDCl_3$ and DMSO-$d_6$, with TMS serving as an internal reference, and chemical shifts were expressed in parts per million. HRMS was recorded on XEVO G2-XS QTOF spectrometer. The absorption and emission studies were conducted on SHIMADZU-2600 machine and the Varian Carey Eclipse Spectrophotometer, respectively. For emission studies, slit widths were set at excitation-10 nm and emission-20 nm at the stated excitation.

**Synthesis of compound 2**[1]

*N*-Bromosuccinimide (2.54 g, 14.28 mmol) was added to a stirred solution of acenaphthene (2 g, 12.98 mmol) in dimethylformamide (20 ml) and the reaction was stirred for 3h at room temperature. The monitoring of the reaction was done with the help of TLC. On completion of reaction, 50 ml of cold water was added to the reaction mixture, and the precipitates formed were filtered and washed with cold water, followed by air drying the precipitate. Brown-colored solid product (**2**) was obtained in 94% yield (2.97 g); $R_f$ 0.6 (hexane); m.pt. 52-55 $^{o}$C.

**Synthesis of compound 3**[1]

Sodium dichromate (10 g) in portion-wise was added to a stirred solution of compound **2** (2 g, 5.58 mmol) in acetic acid at 0 °C, and the reaction was stirred for 25 min at room temperature followed by refluxing for 3h. TLC was used to monitor the reaction, and on completion of the reaction, 40 ml of cold water was added and the formed precipitates were filtered to obtain white solid product (**3)** in 72 % yield (1.75 g); $R_f$ 0.5 (hexane); m.pt. 222-225 °C.

**Synthesis of compound 4**[2]

Sodium azide (0.35 g, 5.38 mmol) was added to a stirred solution of compound **3** (0.5 g, 1.81 mmol) in dimethylformamide:water (9:1) and heated at 100 ºC for 3h. On completion of the reaction, 50 ml of water was poured into the reaction mixture. The precipitates were filtered, and the final product (**4**) was obtained in 75% yield (0.325 g); $R_f$ 0.3 (chloroform: hexane (20:80) m.pt: 230-232 °C.

**Preparation of stock solutions**

The stock solutions of independent anions were prepared in distilled water at a concentration of $1 \times 10^{-1}$ molL$^{-1}$, while the stock solution of **NATRP** was prepared in DMSO:$CH_3CN$ (0.5 mL: 9.5 mL) having a concentration of $10^{-3}$ M. The stock solution of **NATRP** was diluted further to obtain the desired concentration with the required solvent.

**Limit of Detection and Quantum Yield**

We have calculated the fluorescence quantum yield of **NATRP,** the **NATRP-**analyte complex and its AIE features using fluorescein as a standard and its quantum yield is 0.79 in ethanol solution. The formula used is as follows

$$\Phi_S = \Phi_R \times \frac{A_S}{A_R} \times \frac{(Abs)_R}{(Abs)_S} \times \frac{\eta_S}{\eta_R}$$

Where $\Phi_S$ is the quantum yield of sample to be tested, $\Phi_R$ is the quantum yield of the fluorescein; $A_S$ and $A_R$ are the emission band areas of tested sample and fluorescein, $(Abs)_S$ and $(Abs)_R$ are the maximum absorbance values of the tested sample and fluorescein; $\eta_S$ and $\eta_R$ are the refractive index of the solvent used for the sample and fluorescein to record emission band.

The detection limit (DL) was calculated from the following equation:

$$DL = \frac{3 \times standard\ deviation\ of\ blank\ solution}{slope\ of\ calibration\ curve}$$

The quantification limit (LOQ) was determined from the following equation:

$$LOQ = \frac{10 \times standard\ deviation\ of\ blank\ solution}{slope\ of\ calibration\ curve}$$

**Sample preparation for DLS studies**

The prepared stock solution was filtered to remove the suspended particles with the help of 0.02 $\mu$M filter. Zeta potential analyser (ZEN 3600) was used for conducting DLS experiment. The solution having a concentration of 20 $\mu$M was prepared to determine the hydrodynamic size of the particles.

**Field Emission-Scanning Electron Microscopy (FE-SEM) measurement**

The effect of aggregation has been explored by measuring the changes in particle size

and surface morphology using FE-SEM imaging. The **NATRP** solution was placed on a cover slip by drop cast method and allowed to dry for 24 h. The dried sample was subsequently plated with gold spray and FE-SEM analysis was performed. ZEISS MERLIN Compact FE-SEM was used to perform the experiment.

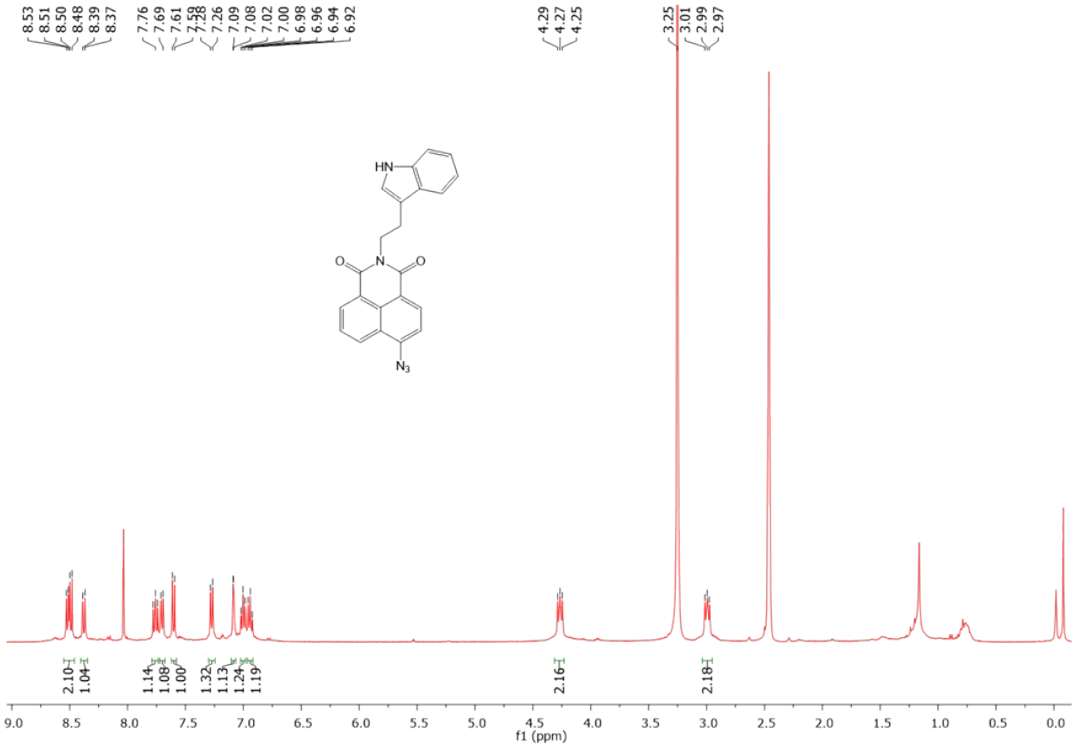


**Figure S1:** $^{1}$H NMR spectrum of 2-(2-(1*H*-indol-3-yl)ethyl)-6-azido-1*H*-benzo[*de*]isoquinoline-1,3(2*H*)-dione

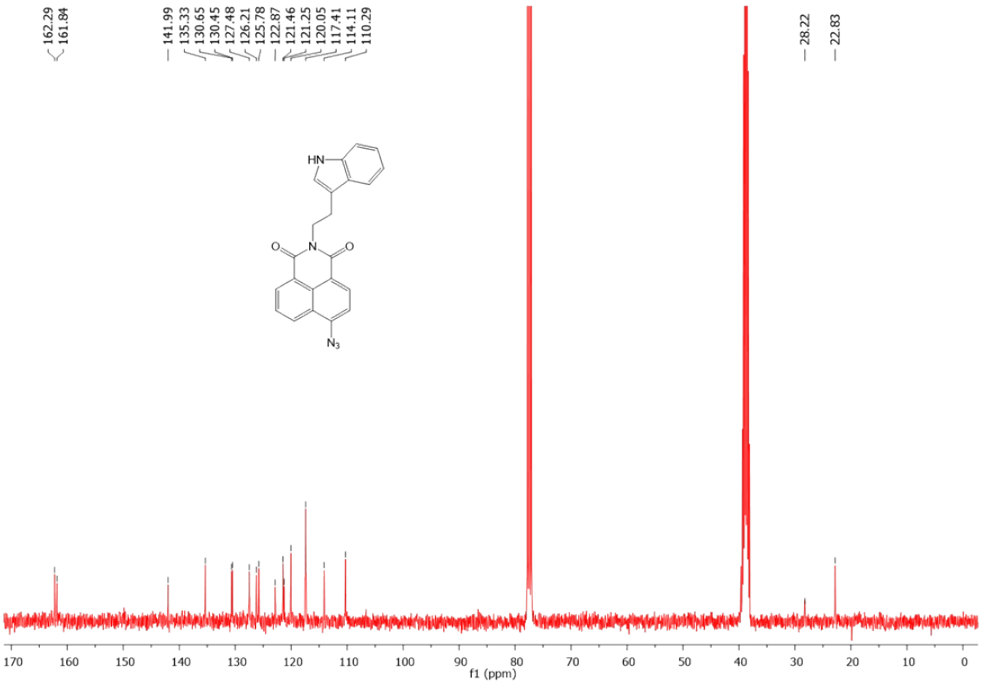

**Figure S2:** $^{13}C$ NMR spectrum of 2-(2-(1*H*-indol-3-yl)ethyl)-6-azido-1*H*-benzo[*de*]isoquinoline-1,3(2*H*)-dione

**Efficiency of NATRP**

The efficiency and performance of **NATRP** to detect $S^{2-}$ ions were also compared with reported sulphide sensors (**Table S1**). According to this data, it is manifested that **NATRP** has significant advantages in being a colorimetric and "Turn-On" sensor with excellent detection limits and rapid sensing of $S^{2-}$ ions within 15 sec than the reported sensors.

**Table S1:** Comparison of present sensor with known sensors

| **S. No.** | **Sensor** | **Solvent System** | **LOD** | **Response Time** | **Application** | **Ref** |
|---|---|---|---|---|---|---|
| 1 | 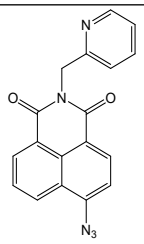 | ACN: $H_2O$ (8:2 v/v) | 1.2 $\mu$M | 10 sec | Bio-imaging | [3] |
| 2 | 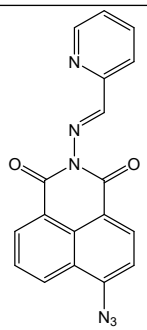 | ACN:$H_2O$ (1:8) | NA | 90 sec | Food samples | [4] |
| 3 | 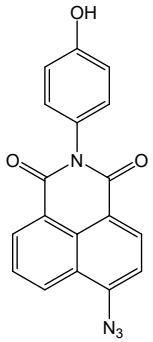 | Phosphate buffer | 50.8 nM | NA | Cell imaging | [5] |

| | | | | | | |
|---|---|---|---|---|---|---|
| 4 | 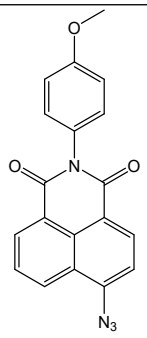 | PBS | 17.4 nM | NA | Cell imaging, detection in red wine | [6] |
| 5 | 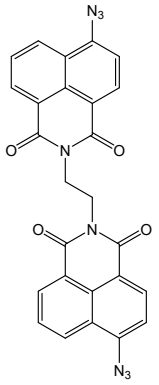 | DMSO:PBS (8:2 v/v) | 0.02 $\mu$M | 150 sec | Cell imaging | [7] |
| 6 | 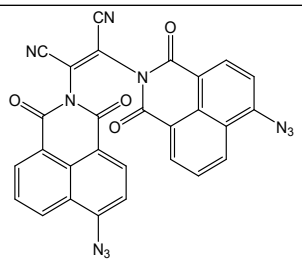 | PBS: DMSO (1:1 v/v) | 1.5 $\mu$M | 10 sec | Cell imaging and real time samples | [8] |
| 7 | 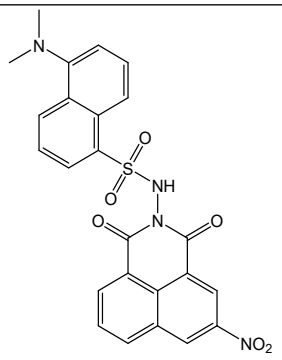 | ACN:$H_2O$ (1:9 v/v) | 0.18 $\mu$M | 30 min | Real water sampling | [9] |
| 8 | 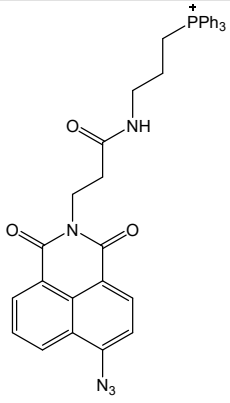 | PBS: DMSO (3:7 v/v) | 1.65 $\mu$M | 5-6 min | Cell imaging | [10] |

| | | | | | | |
|---|---|---|---|---|---|---|
| 9 | 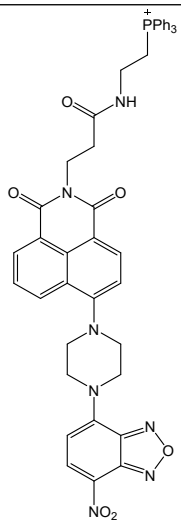 | PBS:ACN (9:1 v/v) | 2.46 $\mu$M | 40 min | Cell imaging | [11] |
| This work | 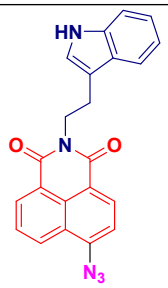 | ACN:$H_2O$ (1:1 v/v) | 7.9 nM | 15 sec | Real water sampling, detection in serum samples, construction of decoder, Cell imaging | This work |

**Computational details**

Initially, compound was optimized at ground state ($S_0$) using B3LYP/6-311G(d) level of theory. All the calculations were carried out using DFT/TD-DFT approach on Gaussian 16. The local minimum character of the obtained structure was confirmed by calculating the vibrational frequencies, as no imaginary value was found for the investigated structures. The IEFPCM model has been utilized to predict the solvation impact of acetonitrile, which was employed to complement the experiment environment. Further, Time-Dependent DFT (TD-DFT) method was used to calculate the excitation energies. The structural optimizations and excitation energy calculations were performed at various functions (BVP86, B3LYP, cam-B3LYP, B3PW91, MPW1PW91, PBE0, and wb97xd); where cam-B3LYP and wb97xd results were found close to experimental findings (**Table S2**).

**Table S2**: Summary of excitation values for first three low lying singlet states in nm at different level of theories for **NATRP**.

| | **BVP86** | **B3LYP** | **cam-B3LYP** | **B3PW91** | **MPW1PW91** | **PBEPBE** | **ωB97XD** |
|---|---|---|---|---|---|---|---|

| | | | | | | | |
|---|---|---|---|---|---|---|---|
| $S_0 \rightarrow S_1$ | 787 | 485 | 333 | 484 | 441 f=0.0008 | 786 | 332 |
| | f=0.0006 | f=0.0006 | f=0.5504 | f=0.0007 | | f=0.0006 | f=0.5583 |
| $S_0 \rightarrow S_2$ | 577 | 391 | 298 | 388 | 362 f=0.4550 | 575 | 286 |
| | f=0.0000 | f=0.0000 | f=0.0010 | f=0.0001 | | f=0.0000 | f=0.0191 |
| $S_0 \rightarrow S_3$ | 491 | 374 | 288 | 372 | 358 f=0.0008 | 484 | 285 |
| | f=0.0000 | f=0.4291 | f=0.0004 | f=0.4322 | | f=0.0000 | f=0.0004 |

Additionally, we have calculated excitation energies using various basis sets at the same level of functional theory (6-311G(d), 6-311G(d,p), 6-311++G(d,p), and cc-pVTZ). When comparing the results, we found a smaller root mean square deviation (RMSD) in atom positions between 6-311G(d) → 6-311G(d,p), and 6-311G(d,p) → 6-311++G(d,p) for the ground state structures. The calculated excitation peak at 332.02 nm for wb97xd/6-311g(d) changes to 332.35 nm for wb97xd/6-311G(d,p); 337.93 nm for wb97xd/6-311++G(d,p), 334.00 nm for wb97xd/cc-pvtz (**Table S3**). The observed small variation in excitation peaks suggested that the 6-311G(d) basis set is sufficient for our study objectives. Therefore, we have utilized wb97xd/6-311g(d) for all further geometry refinement at the excited states.

**Table S3** : Summary of excitation values for three low-lying singlet states in nm at different basis sets of ωB97XD level of theory.

| | **ωB97XD/ 6-311g(d)** | **ωB97XD/ 6-311g(d,p)** | **ωB97XD/ 6-311++g(d,p)** | **ωB97XD/ cc-pVTZ** |
|---|---|---|---|---|
| $S_0 \rightarrow S_1$ | 332 | 332 | 338 | 334 |
| $S_0 \rightarrow S_2$ | 286 | 287 | 290 | 287 |
| $S_0 \rightarrow S_3$ | 285 | 285 | 289 | 280 |

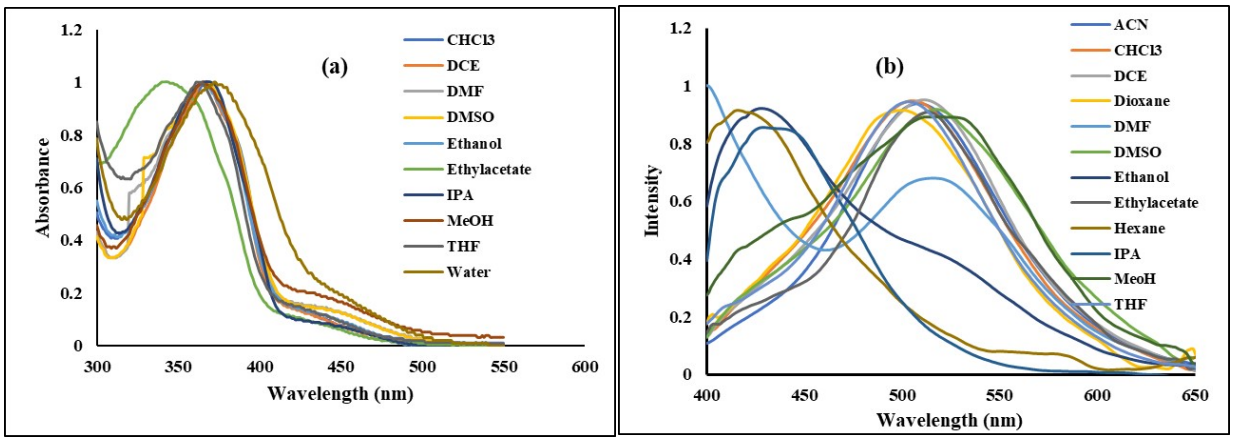


**Figure S3: (a)** Absorption and (b) emission spectra of **NARTP** in various solvents.

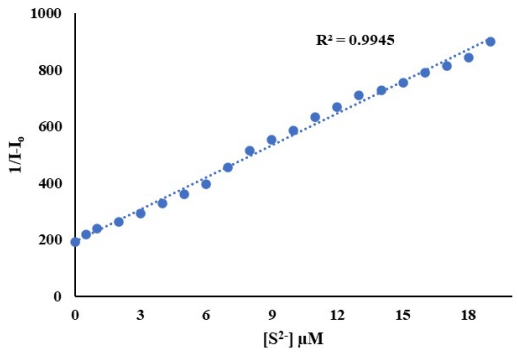


**Figure S4:** Determination of detection limit of $S^{2-}$ by **NATRP** in $CH_3CN$: $H_2O$ (1:1v/v) at $\lambda_{em}$ = 530 nm

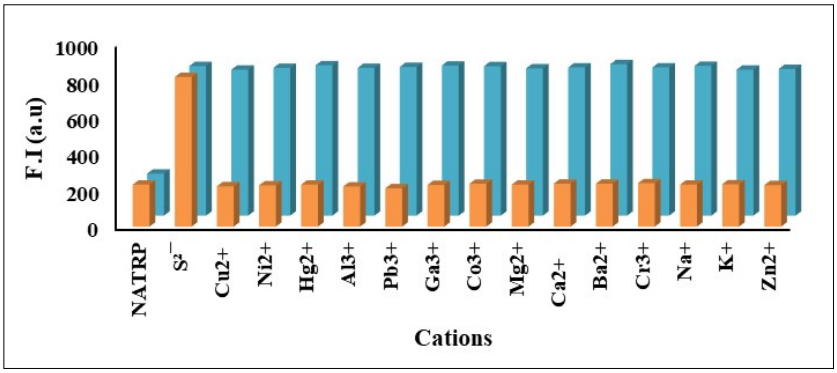


**Figure S5:** Relative emission of **NATRP** (20 $\mu$M) in $CH_3CN$:$H_2O$ (1:1, v/v, *p*H = 7.3), ($\lambda_{ex}$ = 375 nm) with various competing cations in presence and absence of $S^{2-}$ ions at $\lambda_{em}$= 530 nm, in which orange bars show fluorescence intensity change of **NATRP** with various cations (50 eq.) and blue bars show **NATRP** + $S^{2-}$ with other relevant competing cations

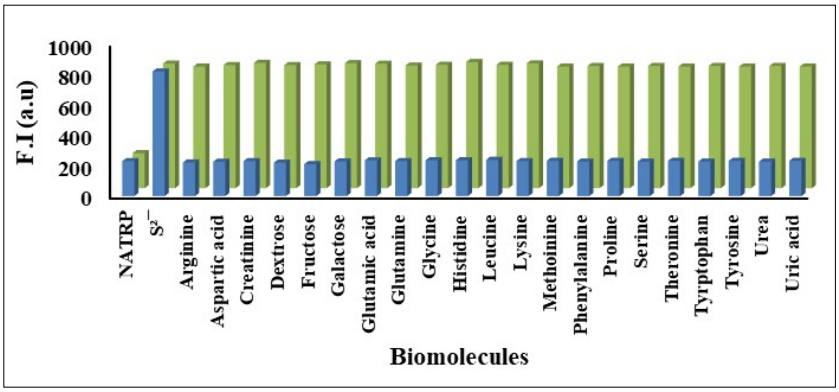


**Figure S6:** Relative emission of **NATRP** (20 $\mu$M) in $CH_3CN$:$H_2O$ (1:1, v/v, *p*H = 7.3), ($\lambda_{ex}$ = 375 nm) with various competing biomolecules in presence and absence of $S^{2-}$ ions at $\lambda_{em}$= 530 nm, in which blue bars show fluorescence intensity change of **NATRP** with various biomolecules (50 eq.) and green bars show **NATRP** + $S^{2-}$ with other relevant competing biomolecules.

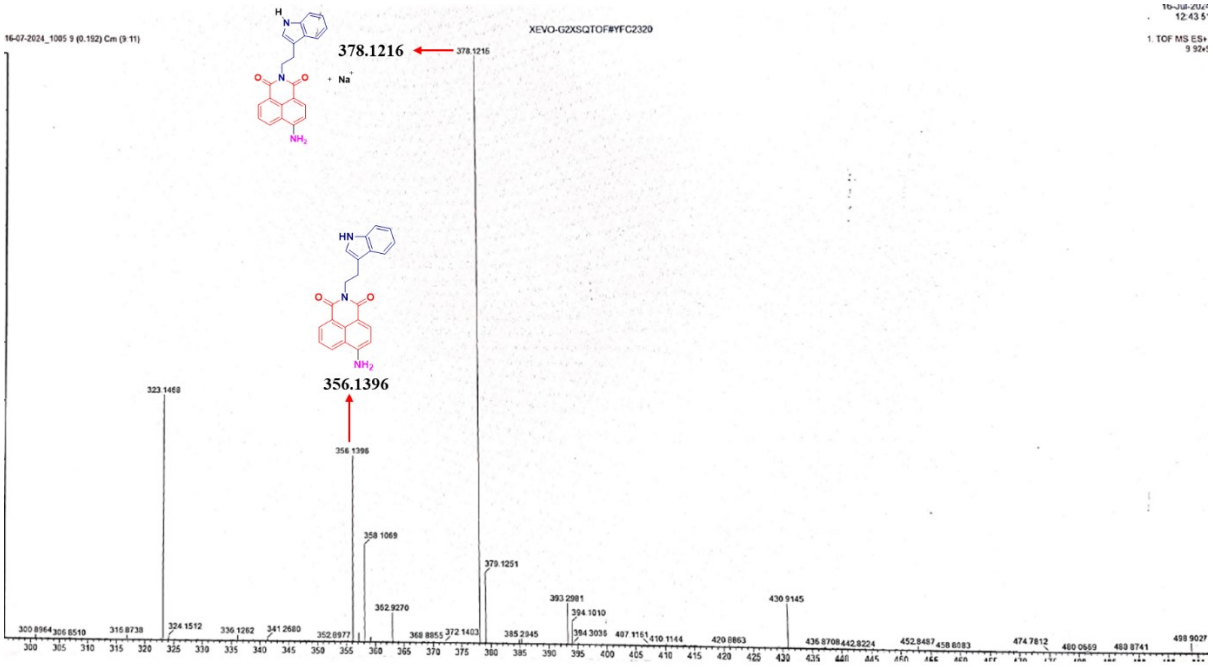


**Figure S7:** HRMS spectrum of **NATRP** in the presence of $S^{2-}$

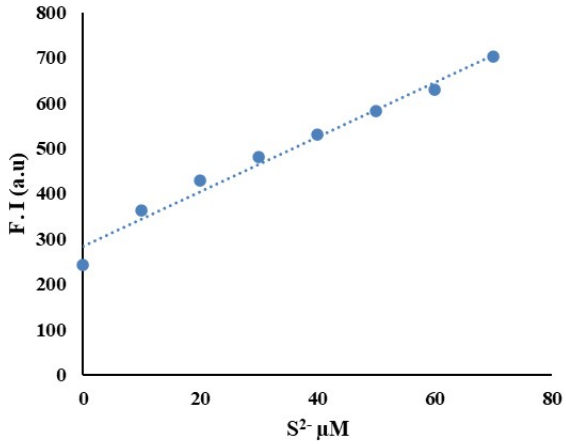


**Figure S8**: Fluorescence spectra of **NATRP** in different concentrations of spiked $S^{2-}$ from 0 to 80 $\mu$M.

**Detection of $S^{2-}$ ions in serum samples**

The healthy concentration of hydrogen sulphide ($H_2S$) in the blood is known to be within the range of 10−100 $\mu$M, and there is a strong relation between serum $H_2S$ level and illness states.[12,13] Therefore, for medical diagnostic purposes, the quantitative detection of $H_2S$ in serum has become much more appealing. We tested the current ratiometric sensor system's to $S^{2-}$ ions in 1% fetal bovine solution in order to assess its possible uses in actual samples. **NATRP** in serum

showed comparatively more fluorescence intensity than in $CH_3CN$: $H_2O$ (1:1 v/v) due to intrinsic $S^{2-}$ ions present in serum. Then, varying concentrations of $S^{2-}$ ions (10, 20, and 30 $\mu$M) were added externally into 1% serum that were treated as real samples. As shown in **Table S4**, the calculated values were in accordance with the added ones, and the recovery was found to be in range, which was adequate for quantitative tests. These findings suggest that the **NATRP** sensor has a potential for monitoring $S^{2-}$ ions in real physiological biofluids.

**Table S4:** Determination of $S^{2-}$ ions in serum sample

| | Added ($\mu$M) | Found ($\mu$M) | Recovery (%) | RSD (%) |
|---|---|---|---|---|
| Serum | 10 | 9.87 | 98.7 | 0.36 |
| | 20 | 21.4 | 107.0 | 0.43 |
| | 30 | 30.4 | 101.3 | 0.40 |

RSD : Relative Standard Deviation

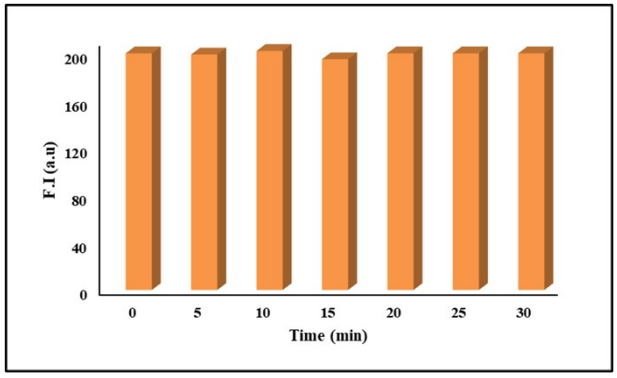


**Figure S9:** Fluorescence intensity of **NATRP** in serum medium with time.

**References**


1. S. Rani, S. Gupta, V. Luxami, K. Paul, *New J. Chem.* **2022**, *46*, 12082–12092.
2. X. Li, Y. Lin, Q. Wang, Y. Yuan, H. Zhang, X. Qian *Eur. J. Med. Chem.* **2011**, *46*, 1274–1279.
3. D. Jothi, S. K. Iyer, *J. Photochem. Photobiol. A Chem.* **2022**, *427*, 113802.
4. A. Ghosh, S. Das, H. S. Sarkar, S. Kundu, P. Sahoo, *ACS Omega* **2018**, *3*, 11617–11623.
5. A Y. Zhang, L. Zhang, *Spectrochim. Acta - Part A Mol. Biomol. Spectrosc.* **2020**, *235*, 118331.
6. Y. Zhang, L. Zhang, *Microchem. J.* **2020**, *159*, 105394.
7. X. Shi, C. Yin, Y. Wen, F. Huo, *Dye. Pigment.* **2019**, *165*, 38–43.
8. D. Jothi, S. Munusamy, S. K. Iyer, *J. Photochem. Photobiol. A Chem.* **2021**, *420*, 113491.
9. S. Das, P. Sahoo, *Sens. Actuators B Chem.* **2019**, *291*, 287–292.

10. B. Deng, M. Ren, J. Y. Wang, K. Zhou, W. Lin, *Sens. Actuators B Chem.* **2017**, *248*, 50–56.
11. Y. L. Pak, J. Li, K. C. Ko, G. Kim, J. Y. Lee, J. Yoon, *Anal. Chem.* **2016**, *88*, 5476–5481.
12. H.D. Li, Q.C. Yao, J.L. Fan, N. Jiang, J.Y. Wang, J. Xia, X.J. Peng, *Chem. Commun.* **2015**, *51*, 16225–16228.
13. H. Peng, Y. Cheng, C. Dai, A. King, L. Predmore, B.L. Lefer, J. Wang, *Angew. Chemie* **2011**, *123*, 9846–9849.